Supporting Information

NIR-to-Visible Upconversion in Quantum Dots via a Ligand Induced Charge Transfer State

Noga Meir[†], Iddo Pinkas[‡], and Dan Oron[†]*.

[†]Department of Physics of Complex Systems, Weizmann Institute of Science, Rehovot 7610001, Israel and [‡]Department of Chemical Research Support, Weizmann Institute of Science, Rehovot 7610001, Israel.

Corresponding Author

*Email: dan.oron@weizmann.ac.il

1. Core/Shell Energy Levels and Exciton Wavefunctions

Energy levels and electron and hole wavefunctions were calculated using effective mass approximation, for 2.8 nm CdSe cores coated with 7 monolayers of CdS (each monolayer ~0.35 nm) and suspended in a solvent with high energy gap. As can be seen in the figure, the hole and electron are localized in the core, however the confinement for the electron is not very strong and it can be found also in the shell.
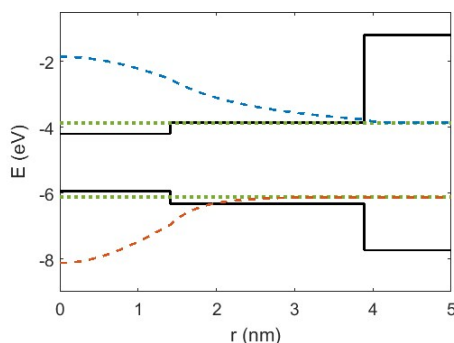

Figure S1 – Energy levels diagram of the core/shell QD, showing the bulk energy levels of the core, shell and solvent (black lines), calculated 1S(h) and 1S(e) energy levels of the core/shell QD (dashed green line), and electron and hole wavefunctions (blue and orange dashed lines, respectively). The x axis denotes the distance from the center of the particle. The energy values are in respect to vacuum.
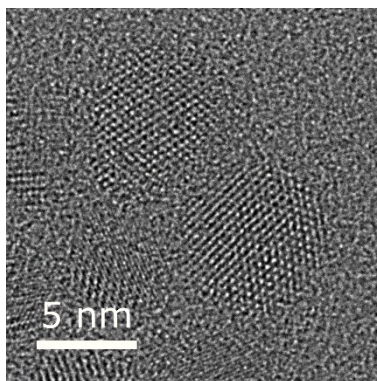
2. HRTEM

Figure S2 – High-resolution TEM image of the core/shell CdSe/CdS QDs

3. Band-Edge Lifetime Fit

The PL data was fit to a biexponential decay trace $\left(A_1 \cdot e^{-\left(\frac{t}{\tau_2}\right)} + A_2 \cdot e^{-\left(\frac{t}{\tau_1}\right)} + c \right)$ convoluted with the measured instrument response, and found that the radiative component of the particles lifetime decreased from 30 to 16 ns following the ligand exchange.
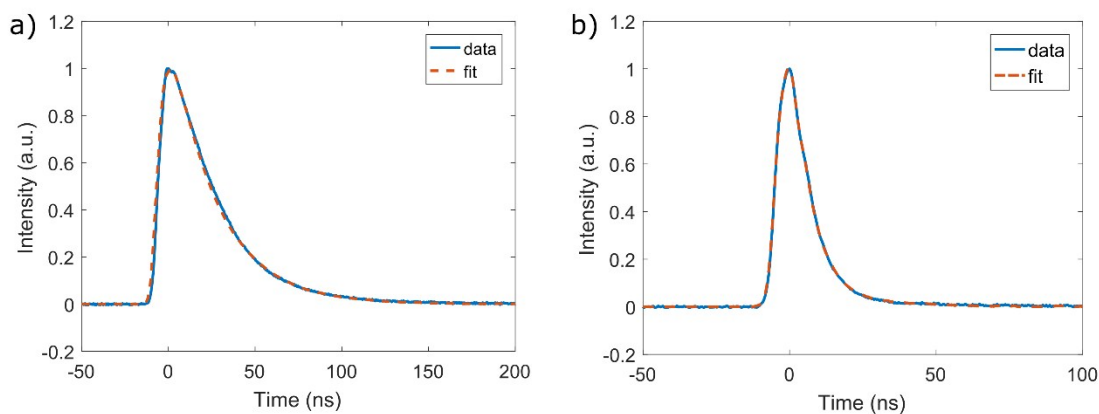

Figure S3 – Typical band-edge emission transient for the QD before (a) and after (b) ligand exchange to TP, obtained at the peak of emission spectrum (570 nm), using 480 nm excitation.
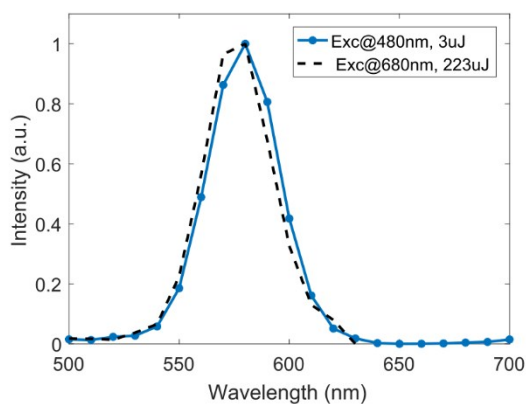
4. UC Spectrum

Figure S4 – Normalized linear (blue) and non-linear (black) PL spectra of the QD-TP, recorded upon excitation at 480 nm and 680 nm, correspondingly.

5. Instrument Response Transient

The instrument response was measured using the reflection of the laser from a cuvette filled with clean toluene, with the same optical setup used for the rest of the photoluminescence measurements. We can clearly see the double pulsing of the beam when approaching the degeneracy point of the OPO (710 nm).
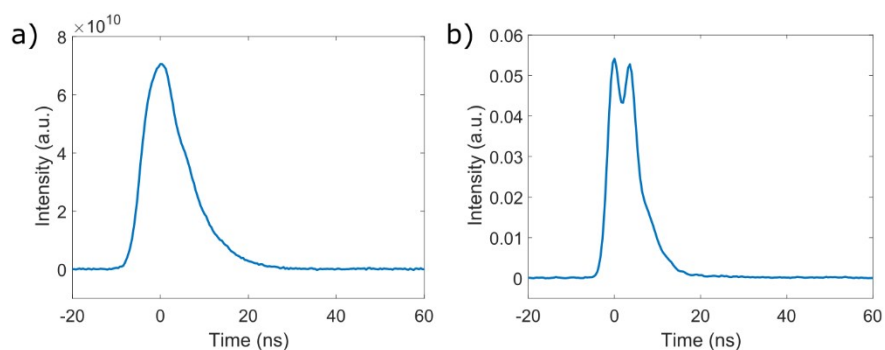

Figure S5 – Time trace of the a) 480 nm and b) 680 nm excitation beam, reflected from clean toluene.
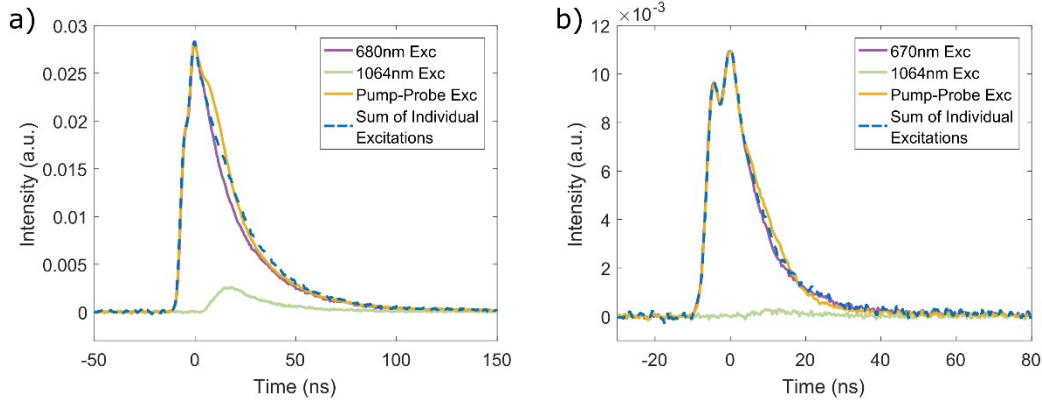
6. Pump-Probe Control Experiment

Figure S6 – a) Typical result of the pump-probe experiment performed on the QDs before the ligand exchange, excited by a 680 nm pump at 115 µJ and a 1064 nm probe at 500 µJ. b) Typical result of a pump-probe experiment performed on the QDs with octanethiol ligands, excited by a 670 nm pump at 70 µJ and a 1064 nm probe at 400 µJ. In both cases we witness no increase of the PL with the arrival of the probe pulse.

7. Qualitative Estimation of Maximal UC

When examining the time-resolved PL signal of the QD-TP system from the pump-probe experiment (Figure 3b, main text), we can see that the non-linear PL is composed of 3 major contributions: the absorption of two red photons resulting from the 670 nm excitations (either simultaneously or sequentially), the absorption of two IR photons resulting from the 1064 nm excitation, and the sequential absorption of one red photon followed by absorption of one IR photon. Thus, the ratio between the PL resulting from the dual excitation and the PL resulting from the two single ones is proportional to:

$$Fl\ ratio \propto \frac{aP_1^2 + P_1P_2 + bP_2^2}{aP_1^2 + bP_2^2}$$

When P_1 is the power of the 670 nm excitation, P_2 is the power of the 1064 nm excitation and a,b are coefficients describing their relative contribution.

Differentiating this expression with respect to the probe power, we get

$$\frac{\partial(Fl\ ratio)}{\partial(P_2)} \propto \frac{\left(P_1 + 2bP_2\right)\left(aP_1^{\ 2} + bP_2^{\ 2}\right) - \left(aP_1^{\ 2} + P_1P_2 + bP_2^{\ 2}\right) * 2bP_2}{\left(aP_1^{\ 2} + bP_2^{\ 2}\right)^2}$$

For weak probe power we get

$$\frac{\partial(Fl\ ratio)}{\partial(P_2)}\bigg|_{P_2 \to 0} \propto \frac{1}{aP_1}$$

So, we expect to see a steeper slope with lower pump power.

The maximal Fl ratio will be obtained when

$$\left(P_1 + 2bP_2\right)\left(aP_1^{\ 2} + bP_2^{\ 2}\right) = 2bP_2\left(aP_1^{\ 2} + P_1P_2 + bP_2^{\ 2}\right)$$

$$P_1 + 2bP_2 = \frac{2bP_2 * P_1P_2}{aP_1^{\ 2} + bP_2^{\ 2}} + 2bP_2$$

$$aP_1^{\ 2} + bP_2^{\ 2} = 2bP_2^{\ 2}$$

$$aP_1^{\ 2} = bP_2^{\ 2}$$

From this condition we can see that as we increase the pump power, the maximal Fl ratio will be obtained at higher probe power values.
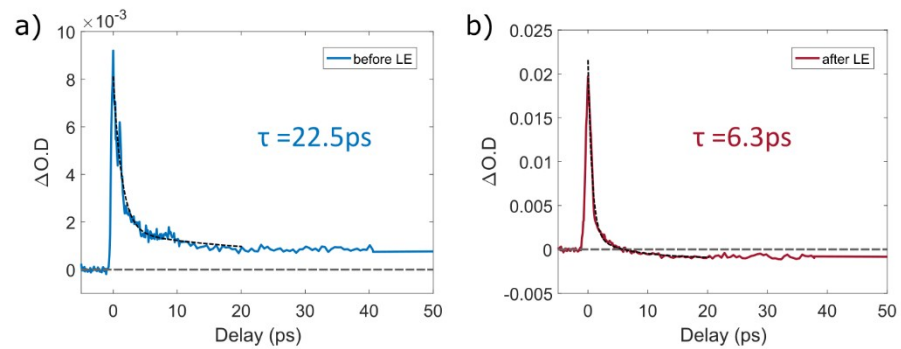
8. TA Kinetics Trace

Figure S7 – ΔO.D. time traces probed around 875 nm for the QDs a) before and b) after the LE, zooming in on the measurements taken with short delays (up to 50 ps). In both traces the carrier cooling dynamics is typical for hole trapping.